# Crystal nucleation and growth from the undercooled liquid: A nonclassical piecewise parabolic freeenergy model

Carey K. Bagdassarian and David W. Oxtoby

Citation: The Journal of Chemical Physics **100**, 2139 (1994); doi: 10.1063/1.466510
View online: http://dx.doi.org/10.1063/1.466510
View Table of Contents: http://scitation.aip.org/content/aip/journal/jcp/100/3?ver=pdfcov
Published by the AIP Publishing

# Crystal nucleation and growth from the undercooled liquid: A nonclassical piecewise parabolic free-energy model

Carey K. Bagdassarian and David W. Oxtoby
*The James Franck Institute, The University of Chicago, Chicago, Illinois 60637*

(Received 7 September 1993; accepted 13 October 1993)

An undercooled liquid exhibits crystalline fluctuations, some of which grow into crystal of macroscopic dimension, while smaller fluctuations disappear. We present a model which allows for exact analytic characterization of the inhomogeneous critical nucleus, the smallest fluctuation which will give rise to crystal growth, in terms of a single spatially varying order parameter for the degree of crystallinity. The model is built around the square-gradient approximation for the free energy with a simple double-parabolic form for the homogeneous component. We study the radius, free energy of formation, and profile of the critical nucleus as functions of the liquid undercooling and compare these with results from an earlier nonclassical theory and from the classical capillarity approximation. The time evolution of the order parameter is described by a phase-field equation which is easily solved numerically for growth dynamics of initially supercritical fluctuations or for the regression of subcritical profiles.

## I. INTRODUCTION

An undercooled liquid is metastable with respect to fluctuations with crystalline structure. If these fluctuations of solid domain are larger than a critical size (called the critical nucleus of the classical capillarity approximation), this new phase will grow at the expense of its undercooled liquid; subcritical clusters, on the other hand, tend to regress to the metastable fluid. More than 40 years ago, Turnbull and Fisher,[1] inspired by the work of Becker and Döring[2] on the appearance of liquid in supersaturated vapor, attacked this problem of nucleation in condensed phases; as such classical formulations prove quantitatively inadequate (for reviews of both classical nucleation theory and modern analogs, see Refs. 3 and 4), workers continue to address the important problem of phase nucleation in both condensed systems and supersaturated vapors.[5–7] Indeed, the recent large-scale molecular dynamics simulations of Swope and Andersen[8] capture beautifully the dynamical process described above, and the work of van Duijneveldt and Frenkel[9] addresses the possibility of nucleation of body-centered cubic crystals instead of the (globally) more stable face-centered cubic structure in melts comprised of spheres interacting with $r^{-12}$ pair potentials.

We propose here a simple model that gives both the spatial profile of the critical cluster, evaluated *analytically* in terms of a single order-parameter description of the solid–liquid interface, and the dynamics of growth or disappearance of initially super- or subcritical nuclei. This is a nonclassical theory, and because the order-parameter profiles and corresponding free energies can be calculated analytically, application of our model should deepen understanding of various nucleation processes. Furthermore, the time evolution of the problem is numerically easily solved. To motivate our formulation, consider briefly the classical picture of nucleation alluded to above. Consistent with the notation which follows, let us write the grand canonical free energy, relative to that of the homogeneous fluid—call it $\Delta\Omega(R)$—for the formation of a spherical solid cluster of radius $R$ as

$$\frac{\Delta\Omega(R)}{\rho_s k_B T_f}=\frac{4}{3}\pi R^3\Delta+4\pi R^2\gamma'. \tag{1}$$

The right side consists of a volume term characterizing the existence of bulk solid and a surface term for the assumed infinitely narrow interface between the spherical solid domain and surrounding liquid. Here $\Delta$ is a dimensionless free-energy difference between bulk crystal and liquid. We ignore any details of crystalline structure and treat the solid simply as a new phase—all we demand is that $\Delta=0$ at solid–liquid coexistence and that $\Delta$ be negative if the liquid is metastable. $\rho_s$ is the density of the solid, $k_B$ is the Boltzmann constant, $T_f$ is the freezing temperature, and $\gamma'\equiv\gamma/\rho_s k_B T_f$, where $\gamma$ is the surface free energy per area for creation of planar interface between crystal and liquid. For an undercooled liquid, $\Delta<0$, and the volume term favors formation of the solid, while the surface term frustrates this nucleation. $\Delta\Omega(R)$ has a maximum $\Delta\Omega^*$ at a critical radius $R^*$—this is the critical nucleus. The limitations of these straightforward ideas are as follows: (1) one cannot simply assume that macroscopic quantities such as surface and bulk free energies can be applied to small, nonmacroscopic clusters, and (2) the surface term ignores the curvature of the interface. In other words, classical nucleation ideas ignore the microscopic structure of the liquid–crystal interface.[10] Nonetheless, the essence of the above picture is clear—a solid fluctuation with radius larger than $R^*$ can decrease the system's free energy only by growing because $d(\Delta\Omega)/dR<0$ in this regime, while a small fluctuation must disappear since $d(\Delta\Omega)/dR>0$ if $R<R^*$. The critical nucleus corresponds to a stationary cluster because infinitesimal fluctuations in its radius will leave the free energy unchanged; i.e., $d(\Delta\Omega)/dR=0$. We are interested then in characterizing the change in radius with time $dR/dt$ as a function of the solid-domain radius,

and it is natural to think of $d(\Delta\Omega)/dR$ as a necessary component of the "driving force" for solid phase dynamics.

Our goal is to understand the above picture with a more realistic scheme which allows for structure in the liquid–solid interface. Assume that the inhomogeneous system can be characterized by a single order parameter $M(\mathbf{r},t)$, which is a function of both space and time. In the bulk liquid $M(\mathbf{r},t)=0$, while the bulk solid has $M(\mathbf{r},t)=M_s$, a positive constant. In other words, we suppress all details of the crystalline lattice and subsume its description under this single order parameter (more will be said about this below). Because $M$ is a structural parameter (we assume that the density difference between liquid and solid has little effect on nucleation rates), it is a nonconserved order parameter, and its time evolution is written in the time-dependent Landau–Ginzburg form[11]

$$\frac{\partial M(\mathbf{r},t)}{\partial t}=-\frac{\Gamma}{\rho_s k_B T_f}\frac{\delta\Omega[M]}{\delta M}. \tag{2}$$

$\Omega[M]$ is the grand canonical free energy, taken to be a functional of the order parameter $M(\mathbf{r},t)$, and its explicit form is discussed below. This expression is reminiscent of the force-flux relations[12] of linear nonequilibrium thermodynamics with $\Gamma$ a transport coefficient, and the functional derivative on the right-hand side has intimate connection to the driving force $d(\Delta\Omega)/dR$ we spoke of in the classical picture. Note that because the system is not in thermal equilibrium, but undercooled with respect to liquid stability, the condition

$$\frac{\delta\Omega[M]}{\delta M}=0 \tag{3}$$

corresponds to the stationary critical nucleus, the cluster with no driving force acting on it, and any deviation from this nucleus will result in time evolution, again in accord with the above classical theory. Equation (3) also corresponds to finding the saddle point of the functional in the usual identification of the critical nucleus.[4] Expressions such as Eq. (2) are also called phase-field equations, as $M(\mathbf{r},t)$ represents the local phase of the material, and have found many applications. Briefly, these kinetic equations guarantee free energy decrease with time, as can be seen by inserting Eq. (2) into the expression for the time change of $\Omega[M]$, which follows from the usual variation of $\Omega[M]$. That is, the quantity

$$\frac{\delta\Omega}{\delta t}=\int d\mathbf{r}\,\frac{\delta\Omega[M]}{\delta M}\frac{\delta M}{\delta t}$$

is always negative when phase-field kinetics are used for $\delta M/\delta t$; for a careful formulation of these ideas, see Ref. 13.

The problem of crystal growth from the melt has received much attention and has a long history (for early work and controversies, see Refs. 14–17). More recently, the dynamics of the process has been reexamined, usually for planar interfaces traveling at steady velocities, with phase-field models variously coupled to thermal diffusion,[18–20] convection in the liquid phase,[21] and solute diffusion in solidification of binary alloys.[22,23] One of us[24] has examined the effects on growth of the anisotropy of the underlying crystal lattice, and time-dependent Landau–Ginzburg expressions have been used in diverse applications to model, e.g., the dynamics of pattern formation in magnetic fluids.[25,26] To the best of our knowledge, the only other work dealing with phase-field models with spherical geometries is the independent study of Caginalp and Socolovsky[27] in which the phase dynamics is coupled to a temperature field. They do examine the question of stability with respect to size change of a critical sphere of solid, but their mathematical/numerical motivation and approach is not the strongly thermodynamic viewpoint we adopt to address the kinetics of growth or regression of spherical crystal fluctuations in undercooled liquids.

Crucial to our development of analytic expressions for the critical profile and simple numerical solutions to the dynamical problem is the choice for $\Omega[M]$, the free-energy functional. As discussed in Sec. II, we use a Cahn–Hilliard square-gradient expression[28] with the local free energy described by two parabolas—one with its minimum at the bulk liquid order parameter, and the other centered on the bulk solid. Section III analyzes the critical nucleus and Sec. IV discusses the evolution to steady-velocity growth of supercritical initial profiles and the rate of disappearance of subcritical ones.

## II. MODEL

A complete theory of crystallization from the melt employs a singlet density

$$\rho(\mathbf{r})=\rho_0\left[1+\eta(\mathbf{r})+\sum_n M_n(\mathbf{r})e^{i\mathbf{k}_n\cdot\mathbf{r}}\right] \tag{4}$$

describing the inhomogeneous solid–liquid system. Here $\rho_0$ is the density of the bulk liquid, $\eta(\mathbf{r})$ is the local fractional density change upon freezing, and the Fourier series represents the periodicity of the crystal with $\{\mathbf{k}_n\}$ the reciprocal lattice vectors. The order parameters of the problem are $\eta(\mathbf{r})$ and the $\{M_n(\mathbf{r})\}$; setting these to zero recovers the bulk liquid density. Harrowell and Oxtoby[10] have used such an expression, eventually retaining only $\eta(\mathbf{r})$ and $M_1(\mathbf{r})$, in a density functional theory, to study the free energy, radius, and shape of the critical nucleus as a function of liquid undercooling. The present model will be simpler. As stated above, we work with the single structural order parameter $M(\mathbf{r},t)$, thereby "enslaving" all other Fourier coefficients to it. Furthermore, we ignore density changes upon crystallization, so there is no need for the $\eta$ parameter. $M(\mathbf{r},t)$ is now a time-dependent quantity, as it will be used to describe evolving order-parameter profiles, with $M=0$ in the bulk liquid phase and $M=M_s$ in the bulk solid. Finally, we assume isothermal crystallization and growth, so the phase-field equation (2) for the order parameter need not be coupled to thermal diffusion. We will be concerned with nucleation and growth (or disappearance) of a spherical crystal, and because crystal anisotropy is ignored (and with it surface stresses that would strain the nucleus), we study the value of $M$ as a function of the radial distance from the center of the sphere; i.e.,

$M=M(r,t)$. Note again that the issues of convection in the liquid phase, heat transport, and crystal structure have been discussed elsewhere in the context of steady growth as listed in Sec. I.

To begin, then, write the free-energy functional of the inhomogeneous solid–liquid system as

$$\frac{\Omega[M]}{\rho_s k_B T_f}=\int d\mathbf{r}\left\{\omega(M(\mathbf{r},t))+\frac{1}{2}K_M^2\left|\nabla M(\mathbf{r},t)\right|^2\right\}, \quad (5)$$

the familiar square-gradient expression of Cahn and Hilliard, where we do not yet need to specialize to spherical symmetry.[28] In this formulation, $\omega$ is a local dimensionless free energy which will characterize a *uniform* system with a degree of order $M$, and $K_M^2$ is the usual coefficient of the square gradient divided by $\rho_s k_B T_f$, making $K_M$ a correlation length for the order parameter. It is the second term of the integral that accounts in an approximate way for the inhomogeneity of the system. When we take the functional derivative of this expression with respect to the order parameter, Eq. (2) for the time evolution of $M(\mathbf{r},t)$ becomes

$$\frac{\partial M(\mathbf{r},t)}{\partial t}=-\Gamma\left[\frac{d\omega(M)}{dM}-K_M^2\nabla^2 M(\mathbf{r},t)\right]. \quad (6)$$

Now, for $\omega(M)$ we choose the suggestive form

$$\omega(M)=\min(\tfrac{1}{2}\lambda_0 M^2,\tfrac{1}{2}\lambda_s(M-M_s)^2+\Delta). \quad (7)$$

These two parabolas, one with its minimum at $M=0$, the bulk liquid value, with curvature $\lambda_0$, and the other centered about the bulk solid with curvature $\lambda_s$, intersect at a special value of $M=M_c$, which is related simply to the dimensionless undercooling $\Delta$. Not only does $\Delta$ shift the "solid" parabola with respect to the liquid, but it is also the free-energy difference between bulk solid and bulk liquid that appears in the classical equation (1). The relationship between the intersection $M_c$ and $\Delta$ is

$$\Delta=\tfrac{1}{2}\lambda_0 M_c^2-\tfrac{1}{2}\lambda_s(M_c-M_s)^2. \quad (8)$$

It is clear that $0\leqslant M(r,t)\leqslant M_s$ for this nonuniform system, and we can anticipate that the center of the sphere is more solid-like, and $M\to 0$ as $r\to\infty$. Thus $M(r,t)$ will serve as an order-parameter profile through the diffuse solid–liquid interface, and there will be a special value of $r=r_c$, where $M$ will pass through $M_c$. That is, when $r<r_c$, $M>M_c$, and we use the solid leg of the free-energy profile (7); when $r>r_c$, $M<M_c$ and the system is "liquid-like." One of our tasks will be to establish the relation between $r_c$ and $M_c$. Because the order-parameter profile is diffuse, it becomes necessary to define an effective radius for the solid fluctuation. It is convenient to use $M_c$ as the special degree of crystallinity defining the boundary between solid and liquid, so that $r_c$ defines the radius of the solid; $dr_c/dt$ then is a measure for the rate of change with time of the radius of the spherical crystallite. (We return to these points below). Finally, we need to say a word on the limits of the dimensionless undercooling $\Delta$. When $\Delta=0$, $M_c=M_s/2$ (if $\lambda_0=\lambda_s$, for the moment) from Eq. (8), and this corresponds to liquid–solid coexistence at equilibrium. This model contains a spinodal at which the liquid loses even its metastability with respect to the solid; here $M_c=0$ and $\Delta_s=-\lambda_s M_s^2/2$ (at this degree of undercooling, there is no longer a parabolic minimum about the bulk liquid). There is no experimental evidence for the existence of the spinodal, so we limit ourselves to

$$-\frac{\lambda_s M_s^2}{2}<\Delta<0 \quad (9)$$

for this nonequilibrium system; and, to be more correct, since we use *linear* kinetic equations, $\Delta$ must be closer to its equilibrium value of $\Delta=0$.

This double-parabola form has been used previously to describe steady-velocity propagation of planar interfaces,[21,29] and its usefulness for the nucleation problem has been recently outlined by one of us,[30] but the model dynamics of spherically growing or shrinking profiles has until now remained unexplored. Independent of our work, Iwamatsu[31] has, with a similar model, characterized the critical nucleus in liquid–vapor nucleation.

## III. THE CRITICAL NUCLEUS

The critical nucleus corresponds to the stationary profile from Eq. (3). Using Eqs. (6) and (7) with specialization to spherical symmetry, we find two ordinary differential equations, as there is no time dependence, for the critical cluster

$$\frac{d^2M(r)}{dr^2}+\frac{2}{r}\frac{dM(r)}{dr}-\frac{\lambda_s}{K_M^2}[M(r)-M_s]=0,$$

$$r<r_c \quad (M>M_c), \quad (10)$$

$$\frac{d^2M(r)}{dr^2}+\frac{2}{r}\frac{dM(r)}{dr}-\frac{\lambda_0}{K_M^2}M(r)=0, \quad r>r_c \ (M<M_c). \quad (11)$$

These inner and outer equations follow directly from using the solid leg of Eq. (7) and switching to the liquid leg at $M=M_c$, the intersection point of the two parabolas. The boundary conditions are simple. We require that the inner solution $M_i(r)$ be well-behaved as $r\to 0$ (i.e., $dM_i/dr\to 0$ as $r\to 0$) and that $M_i=M_c$ at $r=r_c$; for the outer solution, $M_o(r)\to 0$ as $r\to\infty$, and $M_o=M_c$ at $r=r_c$. Furthermore, the derivatives $dM_i/dr$ and $dM_o/dr$ must be equal at $r=r_c$, so that the composite profile $M(r)$ is smooth through all $r$. The solutions are built through positive and negative Yukawas

$$M_i(r)=M_s+\frac{r_c(M_s-M_c)}{r}\times\frac{\exp(-r\sqrt{\lambda_s}/K_M)-\exp(r\sqrt{\lambda_s}/K_M)}{\exp(r_c\sqrt{\lambda_s}/K_M)-\exp(-r_c\sqrt{\lambda_s}/K_M)}, \quad (12)$$

$$M_o(r)=\frac{r_c M_c}{r}\exp\left[-\frac{(r-r_c)\sqrt{\lambda_0}}{K_M}\right]. \quad (13)$$

Equating the derivatives of $M_i$ and $M_o$ at $r=r_c$ gives the relation between $M_c$ (or $\Delta$) and $r_c$; i.e., for a given value of

$r_c$, it is a simple matter to know what undercooling $\Delta$ is necessary to sustain it. The relevant relation is

$$\frac{M_c}{M_s}=\frac{1-[K_M/(r_c\sqrt{\lambda_s})]\tanh[(r_c\sqrt{\lambda_s})/K_M]}{1+\sqrt{(\lambda_0/\lambda_s)}\tanh[(r_c\sqrt{\lambda_s})/K_M]}, \tag{14}$$

and, once again, $r_c$ is a measure of the radius of the spherical crytallite. Two limits are easily obtained from this which are in agreement with intuition. If $r_c\to 0$, $M_c/M_s\to 0$, corresponding to $\Delta\to -\lambda_s M_s^2/2\equiv\Delta_s$; i.e., as the limit of metastability is approached, the liquid is no longer stable even to infinitesimally small solid fluctuations. Recall, however, that this extreme is an artifact of the model and does not appear in the more sophisticated theory of Harrowell and Oxtoby.[10] At the other limit, as $r_c\to\infty$, $M_c\to M_s\sqrt{\lambda_s}/(\sqrt{\lambda_0}+\sqrt{\lambda_s})$, which corresponds to equilbrium or $\Delta=0$, as can be easily verified by insertion of this $M_c$ into Eq. (8), and this is in accordance with the result of Ref. 10.

Note that it is an easy matter to obtain order-parameter profiles as a function of $r$ for various values of $\Delta$. First choose a value of $r_c$ and find the $M_c$ it corresponds to via Eq. (14), and from Eq. (8), the required undercooling. Then use Eq. (12) for the inner solution $M_i(r)$ until $r=r_c$, then continue with the outer $M_o(r)$ of Eq. (13). We defer this treatment until later when we write Eqs. (12) and (13) with dimensionless $r$ and $r_c$ for computational simplicity. We proceed instead to calculate the free energy of formation for critical nuclei. Referring back to Eq. (5), it is clear that the free energy for formation of the critical nucleus, relative to the bulk liquid, is

$$\frac{\Delta\Omega^*_{\rm NC}}{\rho_s k_B T_f}=4\pi\int_0^\infty dr\, r^2\left\{\omega(M(r))+\frac{1}{2}K_M^2\left[\frac{dM(r)}{dr}\right]^2\right\}, \tag{15}$$

where the appropriate $M_i(r)$ or $M_o(r)$ is used depending on the value of the integration variable $r$. The "NC" subscript refers to the nonclassical quantity. The classical quantity corresponding to this is obtained from Eq. (1) with $R$ replaced by $R^*$, the critical radius derived via maximization of $\Delta\Omega(R)$. To continue, Eq. (15) is integrated by parts and written as

$$\frac{\Delta\Omega^*_{\rm NC}}{\rho_s k_B T_f}=2\pi\int_0^\infty dr\left\{2r^2\omega(M(r))-K_M^2 M(r)\frac{d}{dr}\left(r^2\frac{dM}{dr}\right)\right\}, \tag{16}$$

but Eq. (6) reminds us that

$$\frac{r^2}{K_M^2}\frac{d\omega}{dM}=\frac{d}{dr}\left(r^2\frac{dM}{dr}\right) \tag{17}$$

for the critical nucleus, so the working equation is

$$\frac{\Delta\Omega^*_{\rm NC}}{\rho_s k_B T_f}=2\pi\int_0^\infty dr\, r^2\left\{2\omega(M(r))-M(r)\frac{d\omega}{dM}\right\}. \tag{18}$$

Breaking up the range of integration into inner and outer regions separated by $r=r_c$ and using Eq. (7) for the form of $\omega(M(r))$ shows that the outer region does not contribute to the free energy, leaving

$$\frac{\Delta\Omega^*_{\rm NC}}{\rho_s k_B T_f}=\frac{4\pi r_c^3\Delta}{3}+2\pi\lambda_s M_s\int_0^{r_c} dr\, r^2[M_s-M_i(r)]. \tag{19}$$

What follows are straightforward manipulations with $M_i(r)$ given by Eq. (12) and, finally, use of Eq. (14) to remove the resulting $\tanh(r_c\sqrt{\lambda_s}/K_M)$ term in favor of $M_c$ and $r_c$. The final result for the free energy of formation of a critical nucleus is

$$\frac{\Delta\Omega^*_{\rm NC}}{\rho_s k_B T_f}=\frac{4\pi r_c^3\Delta}{3}+2\pi M_s M_c r_c\left(1+\frac{r_c\sqrt{\lambda_0}}{K_M}\right)K_M^2, \tag{20}$$

and this is the barrier to nucleation as a function of undercooling $\Delta$; it represents the free energy of formation for the smallest fluctuation which will grow into a crystal of macroscopic dimension. It is clear that as $r_c\to\infty$, where there is no undercooling, $\Delta\Omega^*_{\rm NC}\to\infty$. At the limit of metastability for the liquid, $r_c\to 0$, and the barrier to nucleation vanishes.

From the above expression, we can extract $\gamma'\equiv\gamma/\rho_s k_B T_f$ the surface free energy for a planar interface that appears in the classical expression (1). Letting $\Delta\to 0$ gives a large crystal domain with locally planar solid–liquid interface, the width of which becomes negligible compared with the crystal radius $r_c$. It is in this regime that the classical free energy becomes valid, and we make the connection between the classical and nonclassical expressions as follows: extremization of Eq. (1) gives for the critical radius

$$R^*=-\frac{2\gamma'}{\Delta},$$

so that, with insertion of this into Eq. (1), we obtain

$$\frac{\Delta\Omega^*}{4\pi R^{*2}\rho_s k_B T_f}=\frac{\gamma'}{3}. \tag{21}$$

Combining this with the nonclassical free energy (20) gives

$$\frac{\gamma'}{3}=\frac{\Delta\Omega^*_{\rm NC}}{4\pi r_c^2\rho_s k_B T_f}=\frac{r_c\Delta}{3}+\frac{M_s M_c K_M\sqrt{\lambda_0}}{2}, \tag{22}$$

since $r_c\to\infty$. Now we need to evaluate $r_c\Delta$ as $r_c\to\infty$ and $\Delta\to 0$. Because $\tanh(r_c\sqrt{\lambda_s}/K_M)\approx 1-2\exp(-2r_c\sqrt{\lambda_s}/K_M)$ for large $r_c$, we can neglect the exponentially decaying term compared with $1/r_c$ and write Eq. (14) as

$$\frac{M_c}{M_s}\approx\frac{\sqrt{\lambda_s}}{\sqrt{\lambda_0}+\sqrt{\lambda_s}}\left(1-\frac{K_M}{r_c\sqrt{\lambda_s}}\right) \tag{23}$$

with

$$1-\frac{M_c}{M_s}\approx\frac{\sqrt{\lambda_0}}{\sqrt{\lambda_0}+\sqrt{\lambda_s}}\left(1+\frac{K_M}{r_c\sqrt{\lambda_0}}\right). \tag{24}$$

These two expressions can be used in the relation between $\Delta$ and $M_c$ given by Eq. (8) to yield, with neglect of terms of $O(1/r_c^2)$, the desired limit

$$r_c\Delta \approx -\frac{\lambda_0\lambda_s K_M M_s^2}{(\sqrt{\lambda_0}+\sqrt{\lambda_s})^2}\left(\frac{1}{\sqrt{\lambda_s}}+\frac{1}{\sqrt{\lambda_0}}\right). \tag{25}$$

Finally, using Eqs. (22), (23), and (25) with neglect of a term of $O(1/r_c)$, we arrive at the surface free energy per unit area

$$\gamma=\frac{\rho_s k_B T_f K_M M_s^2 \sqrt{\lambda_0}\sqrt{\lambda_s}}{2(\sqrt{\lambda_0}+\sqrt{\lambda_s})}. \tag{26}$$

If we start directly with a nonclassical theory for an equilibrium planar interface, we arrive at the same expression. The development is along the same lines as for the spherical case, but note that Eq. (26) differs from Eq. (3-21) in Ref. 21 by a factor of 1/2. The present result is correct.

In order to compare the nonclassical and classical theories and provide plots of the critical profile as a function of the undercooling, it is easiest to rescale our expressions as follows:

$$r\equiv r\sqrt{\lambda_s}/K_M, \tag{27}$$

$$r_c\equiv r_c\sqrt{\lambda_s}/K_M, \tag{28}$$

$$\rho_s\equiv \rho_s K_M^3/\lambda_s^{3/2}, \tag{29}$$

$$R^*\equiv R^*\sqrt{\lambda_s}/K_M, \tag{30}$$

$$\Delta\equiv 2\Delta/\lambda_s, \tag{31}$$

where the variables $r$, $r_c$, $\rho_s$, $R^*$, and $\Delta$ on the right-hand side of these definitions are the ones appearing in the expressions above, and these scalings render $r$, $r_c$, $\rho_s$, and $R^*$ dimensionless. The range of $\Delta$ is now, using Eqs. (9) and (31),

$$-M_s^2<\Delta<0. \tag{32}$$

With these dimensionless quantities, the free energy of the *classical* critical nucleus becomes

$$\frac{\Delta\Omega^*}{\rho_s k_B T_f \lambda_s}=\frac{8\pi}{3\Delta^2}M_s^6\left(\frac{\beta}{1+\beta}\right)^3, \tag{33}$$

while the classical critical radius is

$$R^*=-\frac{2M_s^2}{\Delta}\left(\frac{\beta}{1+\beta}\right) \tag{34}$$

via Eq. (21) and $\beta\equiv\sqrt{\lambda_0/\lambda_s}$. This $\beta$ is a measure of the asymmetries of the free-energy curvatures about the bulk solid and liquid. Iwamatsu[31] proceeds with a similar definition, and understanding the role of $\beta$ will be critical for connection with the earlier work of Harrowell and Oxtoby.[10] For the *nonclassical* critical nucleus, we obtain for the inner and outer order parameter profiles [from Eqs. (12) and (13)]

$$M_i(r)=M_s+\frac{r_c(M_s-M_c)}{r}\frac{\exp(-r)-\exp(r)}{\exp(r_c)-\exp(-r_c)}, \tag{35}$$

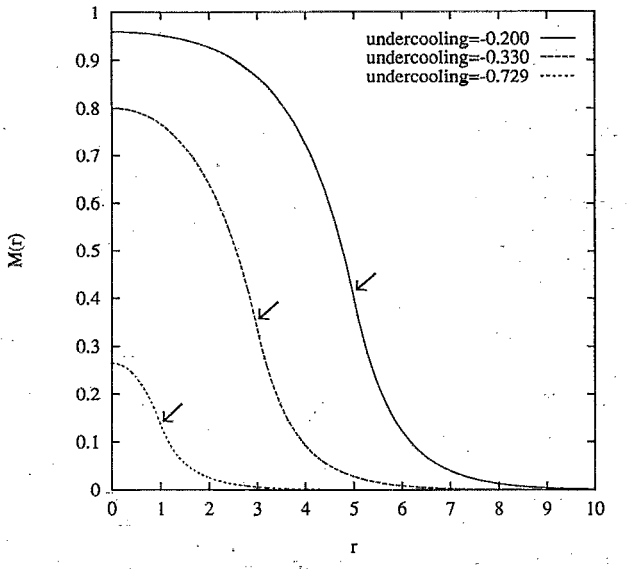


FIG. 1. Order-parameter profile $M(r)$ for three undercoolings. The arrows indicate the positions of $r_c$ for each undercooling.

$$M_o(r)=\frac{r_c M_c}{r}\exp[-\beta(r-r_c)] \tag{36}$$

with the relation between $r_c$ and $M_c$ via Eq. (14)

$$\frac{M_c}{M_s}=\frac{1-(1/r_c)\tanh(r_c)}{1+\beta\tanh(r_c)}. \tag{37}$$

The relation between $M_c$ and $\Delta$ from Eq. (8) is now

$$\Delta=\beta^2 M_c^2-(M_c-M_s)^2, \tag{38}$$

and Fig. 1 shows plots of the order parameter $M(r)$ for three undercoolings. Here, $M_s\equiv 1$ and we have let $\lambda_s=\lambda_0\equiv\lambda$, or $\beta=1$. As the undercooling $\Delta$ decreases, the critical nucleus becomes larger, with the order parameter at the center of the sphere $r=0$ growing toward the bulk solid value of $M_s=1$. To make these plots, we have chosen the radius $r_c$, where we switch from the inner profile to the outer, to be $r_c=1.0$, 3.0, or 5.0, which correspond to $M_c=0.135$, 0.335, or 0.400 and $\Delta=-0.729$, $-0.330$, or $-0.200$, respectively. Note that the interface is diffuse, and if $\lambda=4$ and $K_M=3.4$ Å as in Ref. 21 (though $M_s=0.7$ there), the interfacial width is on the order of 15 Å, in accord with Ref. 10 (the width is much easier to define on plots with smaller undercoolings than shown). Note also that $r_c$ is, indeed, a useful measure of the critical radius as seen from the plots (as is the case for a different choice of $\beta$). Now these plots are simply illustrative of the dependence on undercooling, and we have made no effort to correlate our $\Delta$ with experimentally observed maximum undercoolings for real materials; i.e., it is entirely possible that our largest undercooling cannot be obtained for a given material.

To continue, the free energy for the *nonclassical* nucleus [Eq. (20)] is transformed with the above dimensionless variables to

$$\frac{\Delta\Omega^*_{NC}}{\rho_s k_B T_f \lambda_s} = \frac{2\pi r_c^3 \Delta}{3} + 2\pi M_s M_c r_c (1+\beta r_c). \tag{39}$$

It is important to remember that at the large $r_c$ limit, we equated the classical and nonclassical free energies in Eq. (22). Indeed, as a check one can manipulate Eq. (37) for large $r_c$ in the same way as was done previously, leading to rescaled versions of Eqs. (23) and (24) and use them in Eq. (38) to give

$$r_c \approx -\frac{2M_s^2}{\Delta}\left(\frac{\beta}{1+\beta}\right), \tag{40}$$

which corresponds, in the large $r_c$ limit ($\Delta \to 0^-$), to the classical expression for $R^*$ above. Insertion of this $r_c$ into Eq. (39) and using Eq. (23) to remove $M_c$ leads exactly to the classical free energy of formation. At the other extreme, when $r_c \to 0$ as $\Delta \to -M_s^2$—the spinodal of the model—the nonclassical free energy of formation [see Eq. (39)] goes to zero. Now, the classical expression (33) is positive for this $\Delta$, so that near the spinodal, the nonclassical free energy is less than the classical, independent of $\beta$. Indeed, we can examine $\Delta\Omega^*_{NC}$ and $r_c$ as a function of $\Delta$ as $\Delta \to -M_s^2$ and $r_c \to 0$; Eqs. (37), (38), and (39) yield

$$r_c \approx \sqrt{\tfrac{3}{2}[(\Delta/M_s^2)+1]} \tag{41}$$

and

$$\frac{\Delta\Omega^*_{NC}}{\rho_s k_B T_f \lambda_s} \approx \frac{8\pi M_s^2 r_c^5}{45} \tag{42}$$

near the spinodal. Note that the nonclassical $r_c$ is less than the classical $R^*$ in this limit.

In Figs. 2(a) and 2(b), we plot the critical radius (classical and nonclassical) as a function of the undercooling magnitude $|\Delta|$ with $M_s \equiv 1$. These plots result from Eqs. (34), (37), and (38) with the first for $\beta = 1.0$, and the second $\beta = 0.6$. When the curvature of the liquid and solid free-energy parabolas are the same ($\beta = 1.0$), the classical and nonclassical radii begin to deviate only as the spinodal $|\Delta| = 1$ is approached. When the free-energy curvature about the bulk solid is greater ($\beta \equiv \sqrt{\lambda_0/\lambda_s} < 1$), we see that, as we move away from the spinodal, the nonclassical critical radius, initially smaller than the classical, becomes greater than its classical counterpart. This latter scenario, with $\beta < 1$, is in the spirit of more realistic homogeneous free-energy profiles calculated from density functional theory (see Fig. 1 in Harrowell and Oxtoby).[10] Now, Fig. 4 of their work shows the classical radius to be less than the nonclassical for all supercoolings. We can understand this by realizing that, in their earlier work, there is no spinodal where the liquid becomes unstable with repect to the solid, and the Harrowell and Oxtoby result maps onto the left-hand side of our Fig. 2(b), where $\beta < 1$ (to the region away from our model's spinodal when the nonclassical radius becomes greater than the classical).

Similarly, from Eqs. (33), (37), (38), and (39), we can plot the free energy of formation for a critical nucleus (classical and nonclassical) as a function of $|\Delta|$. These results are shown in Figs. 3(a) and 3(b) where $\beta = 1.0$ and $\beta = 0.6$, respectively. When $\beta = 1.0$, the classical free energy is greater for all $|\Delta|$; when $\beta < 1.0$, there is a crossing at some $|\Delta|$ with the classical free energy less than the nonclassical for smaller undercoolings. This latter regime is in accord with Fig. 3 of Harrowell and Oxtoby with reasoning as above. Note that Iwamatsu[31] compares in a similar fashion the classical and nonclassical pictures for liquid–vapor nucleation.

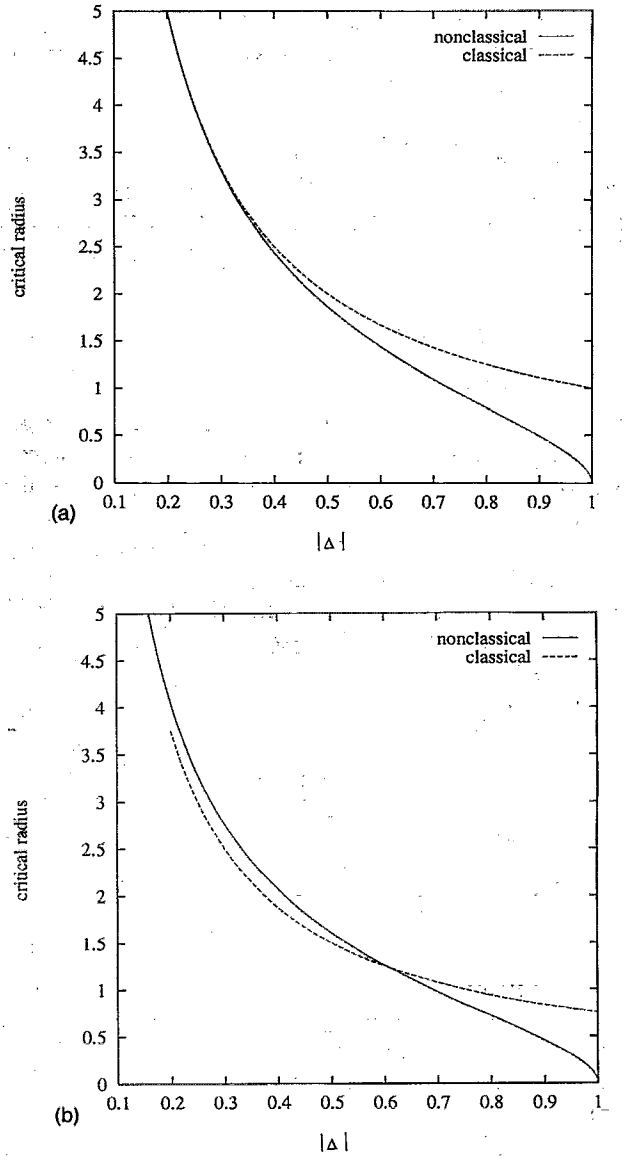


FIG. 2. (a) Critical radius as a function of the magnitude of the undercooling for classical and nonclassical formulations. Here $\beta = 1.0$. (b) The same as in (a), but with $\beta = 0.6$.

## IV. DYNAMICS OF CRYSTAL GROWTH AND DISAPPEARANCE

Finally, we turn to the dynamical aspect of the problem, where the time evolutions are for fixed undercooling, and therefore $M_c$. To write down the differential equations governing the dynamics of order-parameter evolution, we return to Eqs. (6) and (7). We have again inner and outer equations specialized to spherical geometry, with the ex-

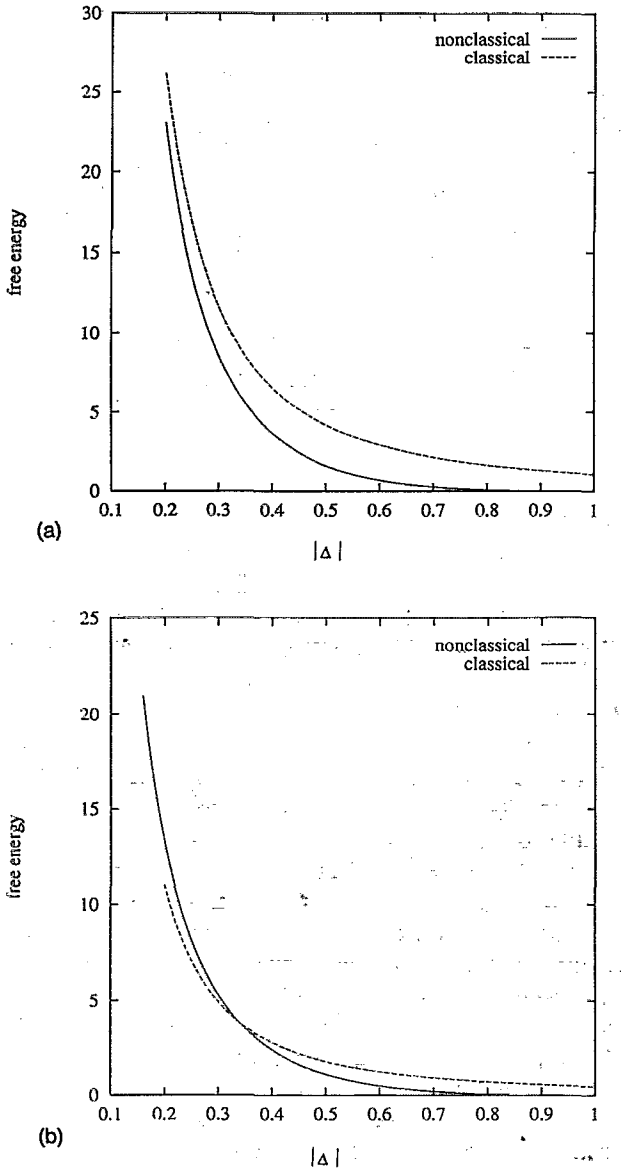


FIG. 3. (a) Free energy of formation for a critical nucleus as a function of the magnitude of the undercooling for classical [Eq. (33)] and nonclassical [Eq. (39)] formulations. Here $\beta=1.0$. (b) The same as in (a), but with $\beta=0.6$.

pressions rendered dimensionless via the rescalings $t\equiv\lambda\Gamma t$ and $r\equiv r\sqrt{\lambda}/K_M$, where for simplicity, $\lambda_0=\lambda_s\equiv\lambda$ [the "$t$" and "$r$" appearing on the right-hand side of these definitions are the variables of the original Eq. (6)]. These kinetic expressions are

$$\frac{\partial M(r,t)}{\partial t}=\frac{\partial^2 M(r,t)}{\partial r^2}+\frac{2}{r}\frac{\partial M(r,t)}{\partial r}-[M(r,t)-M_s], \quad M>M_c, \tag{43}$$

$$\frac{\partial M(r,t)}{\partial t}=\frac{\partial^2 M(r,t)}{\partial r^2}+\frac{2}{r}\frac{\partial M(r,t)}{\partial r}-M(r,t), \quad M<M_c. \tag{44}$$

Recall that $M_c$ is the value of the order parameter where the parabolas of Eq. (7) cross and is constant during the evolution because of the fixed undercooling. Also, because of the rescaling, we do not need to worry at this point about the value of $\Gamma$, the transport coefficient. Now, this $M_c$ is found at some $r_c(t)$—a distance from the center of the solid sphere—which is time dependent since the crystallite will be growing or shrinking if it is not the critical nucleus. This time dependence of $r_c$ determines the rate of crystal growth or disappearance since $M=M_c$ serves as an effective boundary between the solid and liquid regions of our inhomogeneous system—i.e., we follow the dynamics of a chosen degree of crystallinity. The boundary conditions of the problem are similar to those for calculation of the critical profile—the order parameter $M(r,t)$ must be finite at the origin and zero in the bulk liquid for all times with $M_i$, $M_o$, and their first derivatives equal at $r_c(t)$. Indeed, $M_i[r_c(t),t]=M_o[r_c(t),t]=M_c$ at the crystal radius. Finally, we need to provide an initial order-parameter profile so that the problem is well-defined. Note that there is a delicate coupling of the spatial and temporal variables through $r_c(t)$, the point at which the inner and outer solutions must be matched; however, the time evolution of an initial profile is easy to solve numerically.

Consider now the choice for initial profile. We want to maintain connection with the classical idea that an initial supercritical fluctuation will grow while a subcritical one will regress, and we choose a class of initial profiles which is particularly easy to study. We find that crystalline fluctuations growing to macroscopic size via the evolution equations (43) and (44) will approach steady-velocity growth at sufficiently large radii. For subcritical fluctuations, on the other hand, the rate of disappearance will initially increase as the crystallite evolves to smaller size, but as the bulk liquid is recovered, the regression slows. Now it is clear that the critical profile described by Eqs. (35) and (36) (with $\beta=1$) shows no time evolution under Eqs. (43) and (44), but we use as our initial profile

$$M_i(r,0)=M_s+\frac{r_c'(M_s-M_c)}{r}\times\frac{\exp[-(1+K_1)r]-\exp[(1+K_1)r]}{\exp[(1+K_1)r_c']-\exp[-(1+K_1)r_c']}, \tag{45}$$

$$M_0(r,0)=\frac{r_c'M_c}{r}\exp[-(1+K_2)(r-r_c')], \tag{46}$$

where $K_1$ and $K_2$ are two constants describing perturbations around the critical nucleus ($K_1=K_2=0$). The initial radius, call it $r_c'$, at which the switch from the inner evolution equation (43) to the outer evolution equation (44) occurs, is now given by

$$\frac{M_c}{M_s}=\frac{(1+K_1)-(1/r_c')\tanh[(1+K_1)r_c']}{(1+K_1)+(1+K_2)\tanh[(1+K_1)r_c']}, \tag{47}$$

an expression derived, once again, by continuity requirements for the inner and outer profiles at $r_c'$. If Eq. (45) is inserted into Eq. (43) and Eq. (46) is inserted into Eq. (44), it is seen that the initial $t=0$ order-parameter evolution is simply

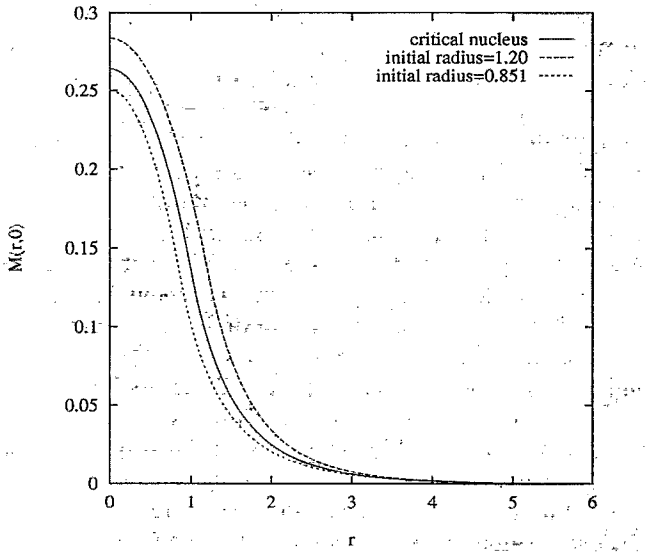


FIG. 4. Perturbations of the critical nucleus at undercooling $=-0.729$. The larger initial profile has $K_1=-0.1$, $K_2=+0.1$, and the smaller initial profile has $K_1=+0.1$, $K_2=-0.1$ in Eqs. (45), (46), and (47).

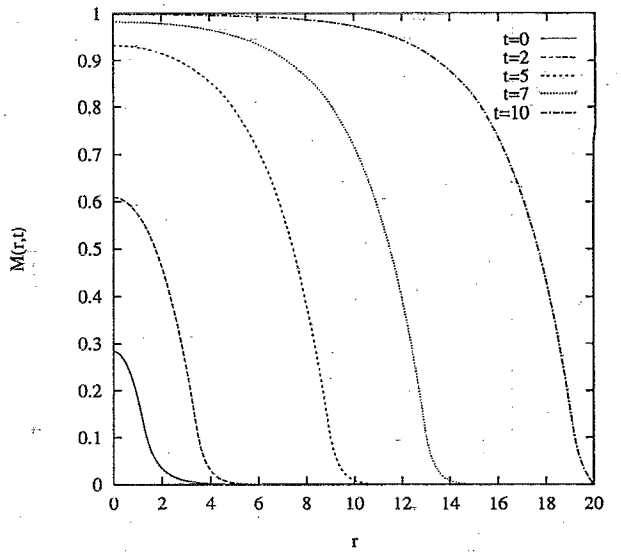


FIG. 5. Growth of an initially supercritical fluctuation with time. The critical nucleus is slightly smaller than the $t=0$ profile as in Fig. 4. See the text for details.

$$\frac{\partial M_i(r,0)}{\partial t}=\frac{r_c'(M_s-M_c)}{r}\times\frac{\exp[-(1+K_1)r]-\exp[(1+K_1)r]}{\exp[(1+K_1)r_c']-\exp[-(1+K_1)r_c']}\times[(1+K_1)^2-1], \tag{48}$$

$$\frac{\partial M_o(r,0)}{\partial t}=\frac{r_c'M_c}{r}[(1+K_2)^2-1]\exp[-(1+K_2)(r-r_c')]. \tag{49}$$

Clearly then, if $K_1<0$ and $K_2>0$, the order-parameter profile is guaranteed to grow initially; for $K_1>0$ and $K_2<0$, the initial fluctuation is shrinking away. This then is the simplicity of our chosen form for the initial crystallite profile. Figure 4 shows the critical nucleus (with $K_1=K_2=0$) when $r_c=1.0$ corresponding to $M_c=0.135$ and two initial profiles at this same $M_c$—one has $K_1=-0.1$, $K_2=+0.1$ with $r_c'=1.20$; the other has $K_1=+0.1$, $K_2=-0.1$, and $r_c'=0.851$. The former crystallite is larger than the critical nucleus and grows, while the latter is smaller and regresses to liquid.

The time evolution of these profiles is an easy matter and is handled nicely by the simplest method of finite differences. First we transform our evolution equations to simpler form. For Eq. (43), let $G(r,t)\equiv r[M_i(r,t)-M_s]$ and let $H(r,t)\equiv rM_o(r,t)$ in Eq. (44). We now have "generic" equations

$$\frac{\partial G(r,t)}{\partial t}=\frac{\partial^2 G(r,t)}{\partial r^2}-G(r,t), \tag{50}$$

$$\frac{\partial H(r,t)}{\partial t}=\frac{\partial^2 H(r,t)}{\partial r^2}-H(r,t). \tag{51}$$

We proceed as follows: the initial profile $M(r,0)$ is transformed to $G(r,0)$ and $H(r,0)$ on a discretized $r$-coordinate with all order-parameter values of $M\geqslant M_c$ (we know the $r$-coordinate where $M=M_c$) going to $G(r,0)$ and those with $M<M_c$ to $H(r,0)$. Note that $M_c$ is transformed both to a $G$ value and an $H$ value as $M_c$ belongs equally to the inner and outer equations; however, the matching of inner and outer profiles, as described below, will take place in the original $M(r,t)$. Now, we propagate in time via Eqs. (50) and (51), as it is simple to transform these equations to the discrete form required by the method of finite differences, and return to $M(r,t)$ to match the two legs of the profile and fit the boundary conditions. Specifically, if $M_c$ is initially at the discrete coordinate $i$, the sites $i-2$, $i-1$, and $i$ with order-parameter values given by the transformation $G$ are used to obtain the value of $G$ at site $i-1$ in the next time step, while sites $i$, $i+1$, and $i+2$ with $H$ values for the order parameter give us $i+1$. When we transform back to $M(r,t)$, we need only ensure that the value of $M$ at $i$ provides for smooth transition between the inner and outer profiles—this amounts to an average of the new $M$ values at $i-1$ and $i+1$. (Of course, the slope of $M$ at the origin is set to zero and $M$ is taken to be the bulk liquid value at $r\to\infty$, in accord with the boundary conditions.) For the next time step, we find the new coordinate with $M=M_c$ and begin again (for growth, the new coordinate will be larger than the original $i$).

Figure 5 shows the growth with time of an initial crystalline fluctuation with $r_c'=1.20$ and $M_c=0.135$ obtained, as before, from Eqs. (45) and (46) with $K_1=-0.1$ and $K_2=0.1$. This corresponds to $\Delta=-0.73$ for the undercooling via Eq. (38), and this initial profile is the supercritical profile of Fig. 4. The maximum elapsed time shown is $t=10$. Note how the order-parameter profile saturates to the bulk solid value of $M_s=1$ with time.

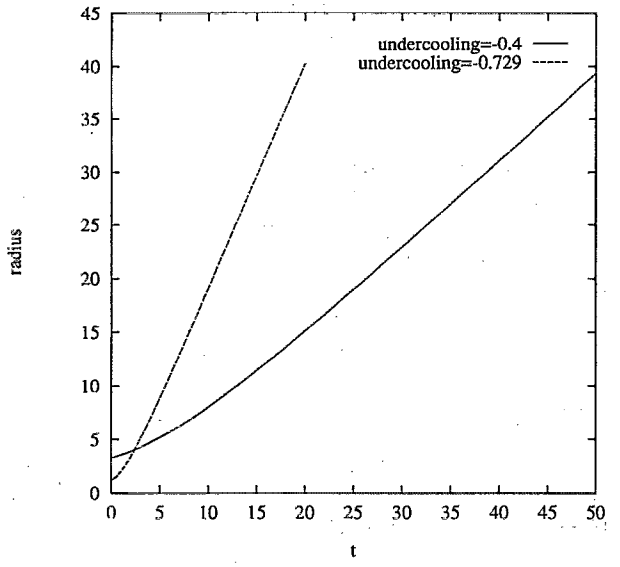


FIG. 6. Growth of the crystalline domain with time for initially supercritical fluctuations. The greater the undercooling, the larger the growth velocity. See the text for details.

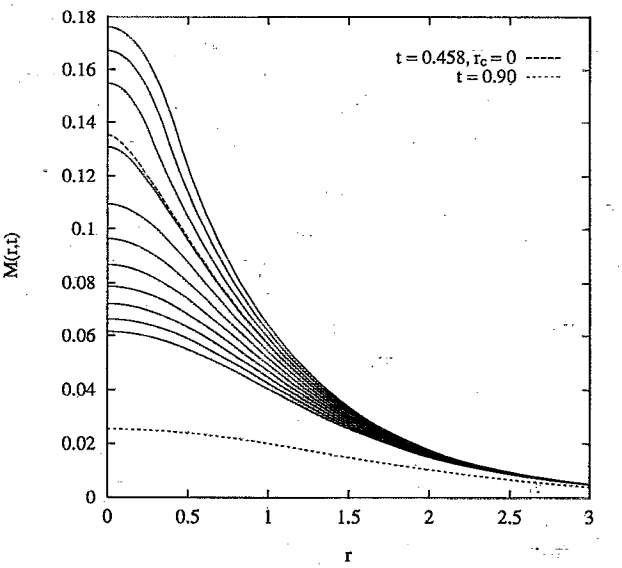


FIG. 7. Dynamics of disappearance for an initially subcritical fluctuation. The largest solid-line profile is for $t=0.40$, and the smallest is for $t=0.60$ with a time interval between profiles of 0.02. The intercalated $t=0.458$ profile represents the crystallite when $r_c \to 0$. The smallest liquid-like profile is at $t=0.90$.

In Fig. 6, we plot the radius of the crystallite domain $r_c$ as a function of time for the above case and for another supercritical profile with $\Delta=-0.4$ and $r_c'=3.30$ initially (here $K_1=-0.1$, $K_2=0.1$ also, and the corresponding critical radius is 2.43). After an initial period of slower growth when the profiles are about the size of the corresponding critical nuclei, note the approach to steady-velocity growth with velocity given by $dr_c/dt \equiv v \approx 2.1$ for the more undercooled case, and $v \approx 0.85$ for the $\Delta=-0.4$ profile (for this latter case, we must evolve the system longer than shown to achieve the steady growth). As a sphere becomes larger with time, the liquid–solid interface becomes planar and the interfacial features become time independent; this means that the driving force for solidification becomes time independent for large times, leading to a steady-growth limit. Indeed, Oxtoby and Harrowell[21] have calculated this steady-velocity growth for a planar interface to be, in the dimensionless units we are using,

$$v=-\frac{2\Delta}{\sqrt{1-\Delta^2}} \tag{52}$$

since the maximum undercooling is $\Delta=-1$ here. For $\Delta=-0.73$, this gives $v=2.1$, and for $\Delta=-0.4$, $v=0.87$, in agreement with our results. Equation (52) makes clear the dependence of the final growth velocity on the undercooling (the greater the undercooling, the greater is $v$) and we can see from our growth scheme that the velocity of crystal propagation is generally smaller if the undercooling is decreased and longer times are required to reach terminal velocity. For $\Delta=-0.73$, the system is in steady growth by $t \approx 20$; if $\Delta=-0.4$, however, only after $t \approx 50$ does a constant velocity begin to set in. Also we can see from Fig. 6 that at $t=10$, $r_c \approx 19$ for the former case, and for the latter, even though the initial fluctuation was larger, at $t=10$, $r_c \approx 8$. It is also important to realize that an initial supercritical fluctuation close in size to the critical nucleus at a given undercooling—i.e., with $K_1$ and $K_2 \approx 0$—will grow with a vanishingly small initial velocity as seen through Eqs. (48) and (49), even if the chosen undercooling is large.

To close this section, we discuss the disappearance of a subcritical fluctuation, the one in Fig. 4, e.g., where $\Delta=-0.73$ and the initial radius is $r_c'=0.851$. Recall that a degree of crystallinity—$M_c$, which is constant—is taken to define the liquid–solid boundary or radius $r_c(t)$ of the fluctuation. When the profile has sufficiently regressed to the point where $M(r,t)$ is everywhere less than $M_c$, we lose our measure of the crystallite radius. Furthermore, as the solid shrinks, $r_c(t)$ moves toward the origin, eventually obviating the need for an inner evolution equation (further evolution requires only the outer equation with suitable boundary conditions). First consider $dr_c/dt$, while $r_c>0$. We stress that even while $r_c$ is approaching the origin, the meaning of a radius becomes obscured because $r_c$ becomes smaller while the crystallite retains considerable spatial extent (but, again, the dynamics are for a chosen crystalline environment described by $M_c$.) With a subcritical fluctuation, then, $dr_c/dt<0$ always. Initially, while the fluctuation is a perturbation of the critical nucleus (for this case, $K_1=0.1$, $K_2=-0.1$), the radius changes slowly, but $|dr_c/dt|$ increases with time so that when $r_c \to 0$, $|dr_c/dt| \to \infty$. Indeed, we can anticipate this result from the form of the evolution equations (43) and (44). If we look at the time change of the order parameter at $r_c$, we see that $\partial M(r,t)/\partial r$ in both equations is negative at $r_c$ and is further divided by $r=r_c$; when $r_c$ becomes small, then, $\partial M(r,t)/\partial t$ has a large negative contribution forcing a rapid change of the spatial position of $M_c$. Figure 7 shows the late-stage evolution of the crystallite. Here $M_c=0.135$ and $r_c \to 0$ with

this value for $M$ at the origin at $t=0.458$ (shown as the fourth curve from the top). The largest profile shown is for $t=0.40$, and the 11 solid-line curves are separated by the same time interval of 0.02. For profiles larger than the intercalated $t=0.458$ curve, evolution proceeds via both inner and outer equations; smaller profiles evolve only under the outer equation (44). When $r_c$ is greater than zero, one sees that $|dr_c/dt|$ certainly does increase as the crystallite shrinks, and this corresponds to a more rapidly changing profile. However, as the crystallite becomes smaller still, its regression to the bulk liquid slows as seen. The smallest profile shown is for $t=0.90$, and note that as the crystallite disappears, it maintains as diffuse a profile as possible.

On a final note, the limit $r_c \to 0$ has a different meaning for the stationary critical nucleus and the shrinking profile just discussed. In the former time-independent case, $r_c$ is controlled by the undercooling as seen, but note that as the undercooling increases, $r_c$, which we have seen to be a good measure of the critical radius, goes to zero with a concommitant loss of crystalline structure because $M_c$ *goes to zero* as well. That is, according to Eqs. (35) and (36), only the outer solution remains relevant as $r_c \to 0$, but this $M_o(r) \to 0$. For the dynamical regression, on the other hand, when $r_c$ becomes zero, we still have a diffuse crystallite sphere because $M_c$ *remains fixed* during the evolution [when $r_c(t)$ reaches the origin, it does so at $M=M_c$].

## V. DISCUSSION

We have characterized, in a nonclassical formulation, the critical nucleus and evolution of sub- and supercritical fluctuations of undercooled liquids. The dynamics are described through a phase-field equation, and a word needs to be said about this. As the subcritical profile evolves to a smaller degree of crystallinity, we have seen that $|dr_c/dt|$ increases and pictorially this increase translates into a more rapidly changing profile as the solid shrinks from the initial fluctuation. Nonetheless, the final regression of the crystallite to the bulk liquid slows. In these final stages, we would expect the dynamics to follow that for regression of fluctuations in a metastable system because our solid region becomes just that—a local fluctuation in order involving perhaps tens of atoms. It remains to be seen whether the phase-field equation can describe the dynamics in these extreme cases of small clusters and how the equation connects with microscopic fluctuation-regression ideas relevant to these metastable systems. Indeed, it becomes necessary to understand how the continuous order-parameter profile $M(r,t)$ translates to the atomic level for a useful measure of the size of these small fluctuations.

To begin to make contact with real materials, at least at the level of our single order-parameter description, we need to match the curvatures of our double parabolas to realistic homogeneous free-energy profiles—our analytic expressions are particularly suited to such manipulations. We saw that introducing a larger relative curvature for the parabola around the bulk crystal qualitatively reproduces the results of Harrowell and Oxtoby. Furthermore, we can extend the model in a straightforward way to more order parameters, again with analytic expressions for the critical nucleus. If we work with two, the density change upon crystallization and a single structural parameter, closer contact can be made to the previous nucleation work; furthermore, Oxtoby and Harrowell have coupled these parameters in the dynamics of steady crystal growth. Finally, generalization to more structural parameters will allow for characterization of nucleation for different lattice types, and we present this work in a future publication.

## ACKNOWLEDGMENTS

C.K.B. has enjoyed many discussions with Dr. Vicente Talanquer, Dr. David Charutz, and Dr. Frank Novak. This work was carried out with the support of the National Science Foundation (Grant No. CHE 9123172) and the NSF Materials Research Laboratories at the University of Chicago.

[1] D. Turnbull and J. C. Fisher, J. Chem. Phys. **17**, 71 (1949).
[2] R. Becker and W. Döring, Ann. Phys. **24**, 719 (1935).
[3] D. W. Oxtoby, J. Phys. Condensed Matter **4**, 7627 (1992).
[4] D. W. Oxtoby, in *Fundamentals of Inhomogeneous Fluids*, edited by D. Henderson (Marcel Dekker, New York, 1992).
[5] (a) H. M. Ellerby and H. Reiss, J. Chem. Phys. **97**, 5766 (1992); (b) C. L. Weakliem and H. Reiss, J. Chem. Phys. **99**, 5374 (1993).
[6] V. Talanquer and D. W. Oxtoby (in preparation).
[7] C. F. Delale and G. E. A. Meier, J. Chem. Phys. **98**, 9850 (1993).
[8] W. C. Swope and H. C. Andersen, Phys. Rev. B **41**, 7042 (1990).
[9] J. S. van Duijneveldt and D. Frenkel, J. Chem. Phys. **96**, 4655 (1992).
[10] P. Harrowell and D. W. Oxtoby, J. Chem. Phys. **80**, 1639 (1984).
[11] N. Goldenfeld, *Lectures on Phase Transitions and the Renormalization Group* (Addison–Wesley, Reading, MA, 1992).
[12] S. R. de Groot and P. Mazur, *Non-Equilibrium Thermodynamics* (Dover, New York, 1984).
[13] O. Penrose and P. C. Fife, Physica D **43**, 44 (1990).
[14] J. W. Cahn, Acta Metall. **8**, 554 (1960).
[15] J. W. Cahn, W. B. Hillig, and G. W. Sears, Acta Metall. **12**, 1421 (1964).
[16] K. A. Jackson, D. R. Uhlmann, and J. D. Hunt, J. Crystal Growth **1**, 1 (1967).
[17] K. A. Jackson, in *Crystal Growth and Characterization*, edited by R. Ueda and J. B. Mullin (North–Holland, Amsterdam, 1975).
[18] S. A. Schofield and D. W. Oxtoby, J. Chem. Phys. **94**, 2176 (1991).
[19] H. Löwen, S. A. Schofield, and D. W. Oxtoby, J. Chem. Phys. **94**, 5685 (1991).
[20] S-L. Wang, R. F. Sekerka, A. A. Wheeler, B. T. Murray, S. R. Coriell, R. J. Braun, and G. B. McFadden (preprint).
[21] D. W. Oxtoby and P. R. Harrowell, J. Chem. Phys. **96**, 3834 (1992).
[22] A. A. Wheeler, W. J. Boettinger, and G. B. Mcfadden, Phys. Rev. A **45**, 7424 (1992).
[23] A. A. Wheeler, W. J. Boettinger, and G. B. Mcfadden, Phys. Rev. E **47**, 1893 (1993).
[24] P. R. Harrowell and D. W. Oxtoby, J. Chem. Phys. **86**, 2932 (1987).
[25] S. A. Langer, R. E. Goldstein, and D. P. Jackson, Phys. Rev. A **46**, 4894 (1992).
[26] A. J. Dickstein, S. Erramilli, R. E. Goldstein, D. P. Jackson, and S. A. Langer (preprint).
[27] G. Caginalp and E. A. Socolovsky, J. Comp. Phys. **95**, 85 (1991).
[28] J. W. Cahn and J. E. Hilliard, J. Chem. Phys. **28**, 258 (1958).
[29] H. Löwen and D. W. Oxtoby, J. Chem. Phys. **93**, 674 (1990).
[30] D. W. Oxtoby, Phys. Scr. (in press).
[31] M. Iwamatsu, J. Phys. Condensed Matter **5**, 7537 (1993).